Pergamon

Journal of Structural Geology, Vol. 16, No. 9, pp. 1327 to 1330, 1994

0191-8141/94 $07.00+0.00

0191-8141(94)E0034-V

Brevia

SHORT NOTES

Refinements to the Fry method (1979) using image processing

LAURENT AILLERES* and MICHEL CHAMPENOIS

Centre de Recherches Pétrographiques et Géochimiques (C.N.R.S.), 15 rue N-D des Pauvres, BP20, 54501 Vandoeuvre, France

(*Received* 8 *November* 1993; *accepted in revised form* 27 *February* 1994)

Abstract—The Fry method is a very powerful way to determine the finite strain ellipse in a deformed rock, but the problems of reproducibility and objectivity of the measurements still remain. Using image processing, the program presented here extracts the central void from Normalized Fry diagrams and computes the characteristics of the best fitted ellipse. It runs automatically on Personal Computers, but remains interactive with the operator, as does the videographic image analyzer.

INTRODUCTION

MANY improvements have been made to the Fry method (1979) since its first application, but the problems of subjectivity and reproducibility still remain. The Fry method for strain determination is a graphical technique. To measure finite strain parameters, one must manually and graphically fit an ellipse on the rim of maximum point density, around the central void presented by the plot. This manual measurement of the axial ratio and the orientation cannot give reproducible results, especially when the central void or the rim of maximum density is not well enough defined.

Erslev & Ge (1990) proposed the Enhanced Normalized Fry method to compute the finite strain ellipse characteristics. Their method consists in the selection of points belonging to an initial Normalized Fry plot (Erslev 1988) and corresponding to certain pairs of neighbour objects. The selection criterion for these pairs of neighbour objects is the value of the "object-pair selection factor" (centre-to-centre distance divided by the sum of the elliptical radii of each object of the pair) which has to be less than a given value, sometimes interactively chosen (Erslev & Ge 1990). The selected points, using the optimal selection factor, determine the rim of maximum density of the initial Normalized Fry plot. Co-ordinates of these points are then introduced in an algorithm which computes the best fitted ellipse using a least-squares method. So, results obtained by this method are dependent on the value given to the selection factor.

The program presented here uses the Normalized Fry method (Erslev 1988), introducing a size parameter to normalize the centre-to-centre distances. This correction eliminates variations due to object size and sorting (Erslev 1988) and improves the definition of the central void. The aim of the paper is to describe an automatic algorithm which allows the objective and reproducible determination of finite strain ellipses, using image analysis.

DATA ACQUISITION AND PROCESSING

Data acquisition

The program runs using digitized files provided by the Interactive Videographic Image Analyzer (Lapique *et al.* 1988) at the C.R.P.G. (Nancy, France). The image analyzer, using a microcomputer, allows the operator to draw superimposed figures on a video image provided by a high resolution video camera. Parameters necessary for the Normalized Fry method (Erslev 1988) are major and minor axes and co-ordinates of the centre of each marker. We propose two ways to extract these parameters. The first consists in the digitization of the two axes assuming grains to be ellipses. The co-ordinates of each centre could then be calculated. The second method consists in the digitization of the whole boundary of the grains. The centre of each marker is calculated as the barycentre of all the points of the grain boundary. The major axis is calculated as the greater length of perpendicular projections of the grain on lines, orientations of which vary from 0 to 180° (greater Feret diameter; Lapique 1987). The minor axis is then calculated by assuming the boundary to be an ellipse,

*Also at Ecole Nationale Supérieure de Géologie, 94 ave De Lattre de Tassigny, BP 452, 540001 Nancy, France.

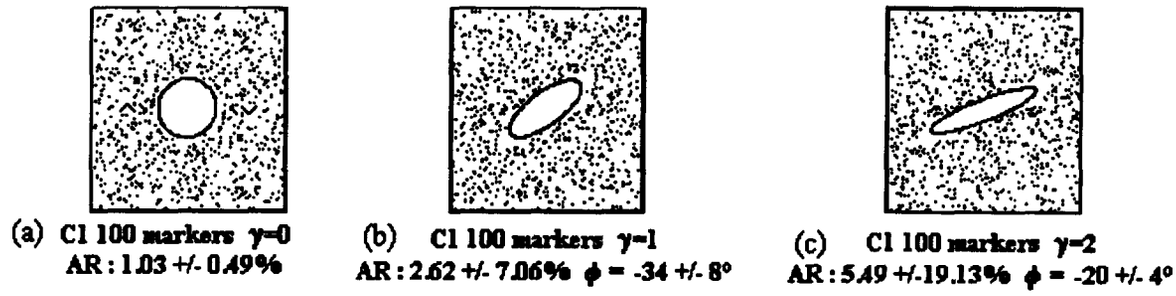

Fig. 1. Normalized Fry diagrams with superimposed ellipse computed for simulated fabrics (sample C1) with increasing shear coefficients (γ) from (a) to (c). AR is for axial ratio.

measuring its area and then dividing this area by a coefficient equal to ($\pi \times$ major axis).

Another problem is the number of objects. The Fry method needs a greater number of markers than is usually obtained by processing of one screen (2×2.58 mm with a magnification of 25) of a thin section under the optical microscope. Since the Normalized Fry method (Fry 1979, Erslev 1988) takes into account the spatial distribution of the markers, we allow the facility to move the section, introducing coefficients of translation corresponding to displacements parallel to X and/or Y of the thin section. This facility greatly improves the results obtained using the Fry method on the analyzer.

Data processing

Using the Normalized Fry method (Erslev 1988), a normalized diagram is computed so that the ratio of switched on pixels to the grid area (100×100 pixels) takes a value between 19.5% and 20.5%. This density (about 20%) has been experimentally determined to approach an image with an optimal definition of the central void. This is automatically obtained by enlargement or reduction of the whole diagram.

The resulting image is submitted to a five-order morphological closing (Serra 1982, Coster & Chermant 1985). A five-order closing consists in the succession of five dilations followed by five erosions. A dilation produces a growth of the initial set due to the result of a "hit and miss" transformation applied on the whole grid (100×100 pixels). The dilation is relative to the intersection between the initial set and a structural element (here, a square mask of $3 \times$ pixels) which is superimposed pixel-by-pixel on the grid. For each position, if one of the 9 pixels in the mask is switched on, the central pixel of the mask will be switched on in the resulting set.

The erosion corresponds to the same scanning of the input set but the central pixel of the mask will be switched on in the resulting set only if the 9 pixels in the superimposed mask are on. This process produces a size reduction of the initial set.

The five-order closing succeeds in switching on all the pixels outside the central void of the diagram. Then, pixels which remain switched off belong to the central void.

CALCULATION OF THE PARAMETERS OF THE FINITE STRAIN ELLIPSE: RESULTS

Using Principal Component Analysis (PCA) on the set of pixels belonging to the central void, the characteristics of the finite strain ellipse are calculated. Using the reference axes of the digitizer, the covariance matrix is calculated. The eigenvector corresponding to the greater eigenvalue gives the orientation of the ellipse, while the square root of the eigenvalues ratio gives its axial ratio.

The preliminary error on pixel positions is equal to $\sqrt{2}$ (in grid unit) corresponding to the square grid. Then, the program computes the finite strain ellipse characteristics for 2 other sets of pixels: (1) initial dilated set, (2) initial eroded set (see above, Serra 1982, Coster & Chermant 1985). So the program gives an uncertainty range for the axial ratio.

Concerning the orientation, the uncertainty range is given by the comparison between the orientation computed using PCA and the orientation measured from the greater Feret diameter (Lapique 1987). These error intervals account for the square grid.

Concerning errors eventually provided by image processing (the five-order closing may make a slight change to the shape of the central void), they are accounted for in part by the uncertainty range, as their calculations are made on both eroded and dilated sets. In other respects, this later eventual source of errors is minimized by the computation method which takes into account all the pixels belonging to the central void and not only its boundary.

EXAMPLES

The process has been tested on simulated fabrics, initially isotropic (Fig. 1a) which are subsequently deformed with different shear coefficients (Figs. 1b & c). The isotropic fabric corresponds to 100 circles of radii between one and two (in arbitrary unit). They are isotropically distributed, they do not overlap each other but are nearly touching. This fabric can correspond to an ideal sedimentary rock, e.g. showing poorly sorted oolites. The two deformed fabrics result from mathematically applying a simple shear matrix to an initial

Table 1. Table of results on simulated fabrics, (a) initially isotropic which have been subsequently deformed with different shear coefficients, (b) uncertainty ranges computed by the program, and (c) relative errors with respect to theoretical values from Lapique (1987). Sample C4 shows no result for $\gamma = 1$ because of the impossibility to determine automatically the finite strain ellipse. γ is for shear coefficient, AR for axial ratio, ϕ for the orientation, C1–C6 are the names of the simulated populations

(a) Table of results

Samples	$\gamma = 0$ A.R.	$\gamma = 1$ A.R.	ϕ	$\gamma = 2$ A.R.	ϕ
C1	1.03	2.62	−34	5.49	−20
C2	1.05	2.32	−30	5.23	−22
C3	1.05	2.31	−31	5.37	−21
C4	1.06	< >	< >	5.43	−21
C5	1.06	2.6	−29	4.62	−20
C6	1.07	2.46	−30	5.49	−22

(b) Table of error intervals computed by the program

Samples	$\gamma = 0$ On A.R. (%)	$\gamma = 1$ On A.R. (%)	On ϕ (°)	$v = 2$ On A.R. (%)	On ϕ (°)
C1	0.49	7.06	8	19.13	4
C2	0.48	3.23	2	10.52	3
C3	0.48	3.03	6	10.15	4
C4	1.89	< >	< >	3.13	4
C5	0.47	4.42	2	10.28	7
C6	1.87	4.07	6	12.11	3

(c) Table of relative errors compared with theoretical values

Theoretical values	1	2.62	−32	5.83	−22
Samples	$\gamma = 0$ On A.R. (%)	$\gamma = 1$ On A.R. (%)	On ϕ (°)	$\gamma = 2$ On A.R (%)	On ϕ (°)
C1	3	0	2	5.83	2
C2	5	11.45	2	10.29	0
C3	5	11.83	1	7.89	1
C4	6	< >	< >	6.86	1
C5	6	0.76	3	20.75	2
C6	7	6.11	2	5.83	0

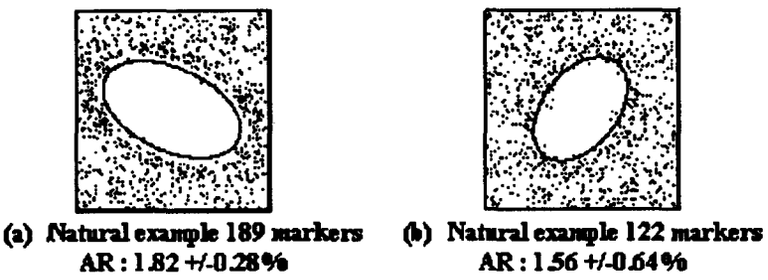

Fig. 2. Normalized Fry diagrams with superimposed elipses computed for natural samples of deformed ironstone oolites: (a) fig. 7.7, and (b) fig. 5.7 of Ramsay & Huber (1983). AR is for axial ratio.

isotropic fabric, with different shear coefficients. The results and the theoretical values are given in Table 1, except for sample C4 with $\gamma = 1$. Results are excellent for shear strain coefficients up to about 2 (axial ratio about 6), but the axial ratios are underestimated for increasing deformation. Note that according to Fry (1979), his method is only valid for axial ratios up to 6. Relative errors (Table 1c) computed with respect to theoretical values are less than 12% (except for sample C5 with $\gamma = 2$), and are reasonable. Concerning the orientation, its determination is always very accurate with absolute errors (Table 1c) less than 3° (in comparison with theoretical values). This error decreases with increasing shear coefficients and axial ratios.

The program has also been tested on natural fabrics in ironstone, oolites (figs. 5.7 and 7.7 from Ramsay & Huber 1983; see Figs. 2a & b). A comparison with their measurements shows nearly identical values. For fig. 5.7 Ramsay & Huber determined an axial ratio of 1.7, using the Rf/Phi method (Ramsay 1967, Dunnet 1969) while the above program computes a value of 1.56. For fig 7.7, they calculated a value of 1.79, whereas our program computes 1.82. These computed values are as accurate a those computed by Erslev & Ge (1990) using the

Enhanced Normalized Fry method (1.567 and 1.641, respectively).

The uncertainty ranges computed by the above program (Table 1b) are very low except for some samples whose central void shape is very complicated, thus introducing higher changes on the central void shape by dilation and erosion processes. Another problem comes from initial Normalized Fry diagrams which present a poorly defined central void (e.g. sample C4 with $\gamma = 1$). The automatic determination of the ellipse is then impossible. We must then interactively and visually fit an ellipse on the Normalized Fry plot, setting the axial ratio, the major axis length and its orientation. For sample C4, results are 2.58 for the axial ratio and $-31°$ for the orientation, which compare well with the known theoretical value (Table 2c).

CONCLUSIONS

The refined Fry method described allows characterization of the whole area of a thin section by the interactive introduction of translation vectors corresponding to the displacement of the section. The digitization technique makes it possible to apply many different methods for the determination of the finite strain ellipse, using either the spatial distribution (Normalized Fry method) as described above or the shape of the grains such as Rf/Phi method (Ramsay 1967, Dunnet 1969) or the Feret diameters method (Lapique 1987).

The program presented here allows the automatic determination of the finite strain ellipse parameters from Normalized Fry plots, but remains interactive with the operator. In case of very high strain (axial ratio over 6) or bad definition of the central void, the operator can adjust the results interactively. The different parameters (axial ratio and orientation) can be changed and the new ellipse is drawn on the initial diagram. In this case, the result is as subjective as the manual fitting of an ellipse on the Normalized Fry plot.

In most cases, corresponding to axial ratios between 1 and 6, the automatic determination is robust. For most samples, the parameters are set to default values (20% for switched-on pixel density in the Normalized Fry diagram and five for the order of closing to extract the central void). That means an objective and reproducible determination of the finite strain ellipse.

Acknowledgements—We would like to thank A. M. Boullier, J. M. Bertrand and J. Macaudière for the very useful discussion and criticisms on this work and the C.R.P.G. (C.N.R.S.) and the E.N.S.G. for their financial supports. We thank also the two reviewers (Dr N. Fry and Dr E. Erslev) and Dr S. H. Treagus for their very useful comments.

REFERENCES

Coster, M. & Chermant, J. L. 1985. *Précis d'analyse d'images*. CNRS, Paris. C.R.P.G. N° 967.

Dunnet, D. 1969. A technique of finite strain analysis using elliptical particles. *Tectonophysics* **7**, 117–136.

Erslev, E. A. 1988. Normalized center-to-center strain analysis of packed aggregates. *J. Struct. Geol.* **2**, 201–209.

Erslev, E. A. & Ge, H. 1990. Least-squares center-to-center and mean object ellipse fabric analysis. *J. Struct. Geol.* **8**, 1047–1059.

Fry, N. 1979. Random point distribution and strain measurement in rocks. *Tectonophysics* **60**, 89–105.

Lapique, F. 1987. Traitement informatique de la déformation finie et interprétation de l'évolution tectonique Pan-Africaine de la région de de Timgaouine (Hoggar, Algérie). Unpublished thèse de l'Université de Nancy I.

Lapique,. F., Champenois, M. & Cheilletz, A. 1988. Un analyseur vidéographique interactif: description et application. *Bull. Minéral.* **111**, 676–687.

Ramsay, J. G. 1967. *Folding and Fracturing of Rocks* . McGraw Hill, New York.

Ramsay, J. G. & Huber, M. I. 1983. *The Techniques of Modern Structural Geology*. Volume 1. Strain Analysis. Academic Press, London.

Serra, J. 1982. *Image Analysis and Mathematical Morphology*. Academic Press, London, 373–423.